CrossMark

TECHNICAL ARTICLE

Developing a method for the evaluation of dislocation parameters from the Rietveld refinement procedure

Saba Khalili,[1] Vishtasb Soleimanian,[1,2,a)] and Ali Mokhtari[1]
[1]*Department of Physics, Faculty of Sciences, Shahrekord University, P.O. Box 115, Shahrekord, Iran*
[2]*Nanotechnology Research Center, Shahrekord University, 8818634141 Shahrekord, Iran*

(Received 27 September 2015; accepted 22 April 2016)

In this investigation, the ability of Rietveld refinement method was used to simultaneously refine the structure and microstructure and evaluate the linear defects of cubic crystals. To do this, the basis of Stephans theory, about the anisotropic strain broadening, was developed and the values of dislocation density as well as the fraction of dislocation types were estimated. The reliability of this procedure was checked by selecting four different nanocrystaslline samples and evaluating the microstructure of these materials. Finally, the results were compared with those extracted from the whole powder pattern modeling method. Good agreement was achieved between the results of two methods. © *2016 International Centre for Diffraction Data.* [doi:10.1017/S0885715616000270]

Key words: X-ray diffraction analysis, Rietveld refinement, microstructure, dislocation parameters

I. INTRODUCTION

The Rietveld refinement is one of the earliest methods of structure characterization based on the whole powder pattern fitting procedure (Rietveld, 1967). Compared with the other line profile analysis approaches, the major advantage of Rietveld refinement is the estimation of phase fractions in the study of alloys, compounds, or mixture of materials (Attallah *et al*., 2009; Ersching *et al*., 2010). Today, the newest packages of this method are provided such that the structure and microstructure characters can be simultaneously refined and extracted from the diffraction patterns (Mojtahedi *et al*., 2013). Although in the anisotropic line broadening these packages can well determine the values of crystallite size and mean square of strain corresponding to various *hkl* reflections, as is known, in only a few Rietveld studies have been evaluated the relation between the anisotropic strain broadening and lattice defects (dislocation characters and planer faults) (Wu *et al*., 1998a; Cerny *et al*., 2000). On the other hand, in several recent papers after determining the crystallite size and mean square of strain from Rietveld refinement, the dislocation density of samples has been estimated (Sarkar *et al*., 2008; Murugesan *et al*., 2012; Rahaei and Jia, 2014; Zhang *et al*., 2015) by using a formula proposed by Williamson and Smallman (1956). The drawback of this equation is that, not only neglecting the effects of slip systems and contrast factor of dislocation, but also considering the contribution of both the size and distortion broadening in dislocation evaluation. However, according to the advanced X-ray diffraction line profile analysis the dislocations can only affect the anisotropic strain broadening and they have no influence on the broadening of size (Ungar *et al*., 1999a; Dragomir and Ungar, 2002).

It seems that if, instead of the old X-ray method, the newer theories of line profile analysis are combined with the Rietveld refinement procedure, it can be more accurately studied the influence of structure and microstructure characters on the mechanical, chemical, or physical properties of materials. In this work, the basis of anisotropic strain broadening formulated by Stephens in Rietveld method (Stephens, 1999) is incorporated to the modified form of Caglioti equation proposed by Wu *et al*. (1998a). The result is compared with the relation between the contrast factor of dislocation and fourth-order invariant coefficients, reported by Ungar and Tichy (1999b). This procedure can estimate the fraction of edge/screw dislocation types and dislocation density in cubic system.

In order to check the reliability of the Rietveld method, the X-ray diffraction data were tested for four different samples. The first two materials, prepared by the top-down nanofabrication technique are the mechanical alloying of elemental copper/iron and aluminum powders. The other materials, selected from the bottom-up method of nanoparticle preparation, are the nanocrystalline MgO powder and CdO thin films. Both of them were synthesized by sol–gel method. The crystallite size, dislocation density, and the fraction of edge/screw dislocation types corresponding to these samples were determined by Rietveld refinement. In CdO samples, the behavior of these microstructure parameters was evaluated as a function of annealing temperature. Finally, the results were compared with those achieved by one of the powerful methods of microstructure evaluation, i.e. whole powder pattern modeling (WPPM) procedure (Scardi and Leoni, 2002).

II. RELATION BETWEEN THE RIETVELD RESULTS AND DISLOCATION PARAMETERS

The structure and microstructure parameters can be evaluated using the space group, the initial values of lattice parameters and the position of atoms in lattice, corresponding to each phase of tested material as the input values of Rietveld software packages (Rodriguez, 1990; Ferrari and Lutterotti, 1994). The location as well as the approximate intensity of reflections in the diffraction patterns are estimated from the structure factor of each phase. The width of peak profiles is

a)Author to whom correspondence should be addressed. Electronic mail: soleimanian@sci.sku.ac.ir

https://doi.org/10.1017/S0885715616000270 Published online by Cambridge University Press

usually the linear or non-linear combination of the breadth of Lorentzian (H_L) and Gaussian (H_G) functions. For microstructure determination, by applying the Thompson–Cox–Hastings pseudo-Voigt function, the breadth of peak profiles (H_K) is taken from the following equation (Solovyov, 2000):

$$H_K^5 = H_G^5 + 2.69269H_G^4H_L + 2.42843H_G^3H_L^2 + 4.47163H_G^2H_L^3 + 0.07842H_GH_L^4 + H_L^5, \ldots \quad (1)$$

where H_G and H_L can be determined using Eqs. (2) and (3).

$$H_G^2 = U\tan^2\theta + V\tan\theta + W + \frac{I_G}{\cos^2\theta} \quad (2)$$

$$H_L = X\tan\theta + \frac{Y}{\cos\theta} \quad (3)$$

During the fitting procedure, the values of U, V, W, I_G, X, and Y as well as the structure parameters must be refined until minimizing the difference between the calculated and observed patterns. Now the volume (D_V) and area (D_A) weighed crystallite size can be determined in addition to the apparent size (D) and the mean square of strain $\langle e^2\rangle^{1/2}$ by using Eqs. (4)–(7) (Rodriguez, 1990):

$$D_V = \frac{1080\lambda}{\pi^2}\left[2(Y-Y_S) + \left[(Y-Y_S)^2 + \frac{9}{\pi^2 Ln2}(Z-Z_S)\right]^{1/2}\right]^{-1} \quad (4)$$

$$D_A = \frac{180\lambda}{\pi^2}(Y-Y_S)^{-1} \quad (5)$$

$$D = D_A + \frac{(D_AD_V)^{1/2}}{4} \quad (6)$$

$$\langle e^2\rangle^{1/2} = \frac{1}{12}\left(\frac{\pi^2}{360}\right)\left[2(X-X_S) + \left[(X-X_S)^2 + \frac{9}{\pi^2 Ln2}(U-U_S)\right]^{1/2}\right]^{-1} \quad (7)$$

where Y_S, Z_S, X_S, and U_S are the coefficients corresponding to the peak profiles of instrumental sample.

It should be noted that, since in most of the nanocrystalline materials the density of linear defects is very high, the strain of various *hkl* reflection has no unique value. In this case, which are named anisotropic strain broadening, U and X parameters in Eqs. (2) and (3) must be changed to $U + (1-\zeta^2)\sigma^2(M)/M^2$ and $X + \zeta\sigma(M)/M$. In cubic crystals, according to the Stephens model, $M = h^2+k^2+l^2$ and $\sigma(M)$ are obtained from the following equation (Stephens, 1999):

$$\sigma^2(M) = S_{400}(h^4+k^4+l^4) + S_{220}(h^2k^2+h^2l^2+k^2l^2) \quad (8)$$

in which, S_{400}, S_{220}, and ζ, in anisotropic strain broadening, are also the refinable parameters during the fitting procedure.

Moreover, according to Wu *et al.* (1998a, 1998b), in the dislocated crystals the relationship between the breadth of Gaussian components and the contrast factor of dislocations ($\overline{C}_{hkl}$) can be given as:

$$H_G^2 = (U + T\chi)\tan^2\theta + V\tan\theta + W + \frac{I_G}{\cos^2\theta} \quad (9)$$

where $\chi = \overline{C}_{hkl}b^2$, b is the Burgers vector, and T is a parameter related to the refinable anisotropic strain broadening parameters. The relation between Lorentzian component and strain broadening is more complicated and therefore in this research only the Gaussian component was applied. Thus, the following equation can be derived by substituting the new form of U (in anisotropic strain broadening case) into Eq. (9):

$$T\chi = T\overline{C}_{hkl}b^2 = (1-\zeta)^2\frac{s_{400}(h^4+k^4+l^4) + s_{220}(h^2k^2+h^2l^2+k^2l^2)}{(h^2+k^2+l^2)^2} \quad (10)$$

On the other hand, according to Ungar and Tichy (1999b), in cubic crystals the average contrast factor can be expressed as the fourth-order polynomials of *hkl* indexes:

$$\overline{C}_{hkl} = A + BH^2 \quad (11)$$

where

$$H^2 = \frac{h^2k^2+h^2l^2+k^2l^2}{(h^2+k^2+l^2)^2} \quad (12)$$

The average contrast factor can also be written as the fractions of edge (η_e) and screw (η_s) dislocation characters as:

$$\overline{C}_{hkl} = \eta_e\overline{C}_{hkl,e} + \eta_s\overline{C}_{hkl,s} = \eta_e\overline{C}_{hkl,e} + (1-\eta_e)\overline{C}_{hkl,s} \quad (13)$$

In the above equation, $\overline{C}_{hkl,e}$ and $\overline{C}_{hkl,s}$ are the average contrast factors corresponding to edge and screw dislocation types, respectively. Combining Eqs. (10) to (13), the following equation is obtained:

$$Tb^2[(\eta_eA_e + \eta_sA_s) + (\eta_eB_e + \eta_sB_s)H^2] = (1-\zeta)^2[S_{400} + (S_{220} - 2S_{400})H^2] \quad (14)$$

or

$$\frac{\eta_eA_e + \eta_SA_S}{\eta_eB_e + \eta_SB_S} = \frac{S_{400}}{S_{220} - 2S_{400}} = K' \quad (15)$$

Finally, the fractions of edge dislocation characters can be determined from the refinable parameters S_{400} and S_{200} as:

$$\eta_e = \frac{K'B_S - A_S}{A_e - A_S + K'(B_S - B_e)} \quad (16)$$

In order to determine the dislocation density (ρ), according to the approach proposed by Cerny *et al.* (2000), the relation between the mean square of strain and density of dislocation is as

https://doi.org/10.1017/S0885715616000270 Published online by Cambridge University Press

follows:

$$\langle e^2\rangle_{hkl} = \frac{\rho}{8}\Lambda^2(\ln P)\overline{C}_{hkl}b^2 \quad (17)$$

where

$$\Lambda = \left(1 - \frac{\ln(\ln P)}{4\ln P}\right)^{-1} \quad (18)$$

and P, which is the dislocation correlation parameter, can be approximately determined from the ratio between the Lorentz (β_L) and Gauss (β_G) integral breadth:

$$P \simeq 3(\pi \ln 2)^{-1/2}\frac{\beta_G}{\beta_L} \quad (19)$$

Now according to Eq. (17), the mean value of dislocation density can be determined from the slop of the plot of $\langle e^2\rangle_{hkl}$ vs. $\xi_{hkl} = \Lambda^2(\ln P)\overline{C}_{hkl}b^2/8$. It is important to point out that, since the anisotropic microstructure section of Fullprof software has been written on the basis of the Stephens model (Stephens, 1999) and can be completely adopted to all of the above assumptions, in our work, this software was selected from among the various Rietveld packages.

III. TESTING THE FORMULA ON CUBIC NANOMATERILAS

A. Materials preparation

In order to test the procedure explained in the previous section, four different cubic materials were selected. The mechanically alloyed nanocrystalline Fe–Cu (sample S_1) and deformed aluminum powders (sample S_2), were prepared by planetary ball-mill. In sample S_1, the weight fractions of Fe and Cu were equal and the milling time of samples S_1 and S_2 was set to 12 and 48 h, respectively. Further details were reported in our previous works (Mojtahedi *et al.*, 2013; Soleimanian and Mojtahedi, 2015).

The nanoparticle of magnesium oxide (sample S_3) was synthesized using the sol–gel technique. In this process, the sodium hydroxide and magnesium nitrate were used as the starting materials. After preparing the MgO nanopowder, it was annealed in air for 2 h at 600 °C (Soleimanian *et al.*, 2015).

The last material, attempted to more systematically explain in this research, is the thin film of cadmium oxide (samples S_4–S_8). To deposit the CdO nanoparticles on the ordinary glass slide substrates, the sol–gel spin coating method was applied. The cadmium acetate, 2-methoxiethanol, and monoethanolamine were used as the source of cadmium, solvent, and stabilizer, respectively. The prepared gel was dropped onto the cleaned substrates, the films were rotated at 1000 rpm for 30 min, and dried at 150 °C. After repeating the spin coating drying cycles, the films were annealed at 300–500 °C in air (Yahia *et al.*, 2013).

The X-ray diffraction data of samples were measured by Philips PW-1840 and Panalytical X'Pert Pro MPD, diffractometers, using Co$K\alpha$ (λ = 1.789 Å) and Cu$K\alpha$ (λ = 1.541 Å) radiations, respectively. The properties of angular range, step size, step counting time, divergence slits, goniometer radius, and detector types are given in Table I. In order to apply the effect of instrumental broadening, the Al_2O_3 and La_2B_6 powders with large crystallites and negligible strain were used as the standard samples of first and second diffractometers, respectively. The X-ray diffraction patterns of samples S_4, S_6, and S_8 are shown in Figure 1 [the diffraction profiles of S_1 to S_3 were previously reported in (Mojtahedi *et al.*, 2013; Soleimanian and Mojtahedi, 2015; Soleimanian *et al.*, 2015)].

B. Rietveld refinement procedure

Before any analysis, the behavior of peak profile broadening corresponding to each sample should be investigated. This feature can be observed in the Williamson–Hall plot by analyzing the variation of integral breadth in reciprocal space (β^*) vs. the diffraction vector (g) (Williamson and Hall, 1953). Figure 2 shows the Williamson–Hall plots of Cu (S_1), Al (S_2), MgO (S_3), and CdO (S_4–S_8) phases. As is seen the β^* is not a monotonous function of g and the strain anisotropy, observed in the plots must be evaluated vs. linear defects. It should be noted that the Williamson–Hall plot of Fe phase (sample S_1) only has three points and therefore the behavior of line broadening cannot be evaluated for this phase.

To simultaneously investigate the structure and microstructure properties, the space group, the position of atoms, and the initial values for lattice parameter of each sample were separately used in Fullprof software (Rodriguez, 1990). The background parameters, lattice constants, and the coefficients of Eqs. (2) and (3) were then refined and the measured X-ray diffraction patterns were fitted to the calculated one, using Thompson–Cox–Hastings pseudo-Voigt function. But as is shown in Figure 3(a), the quality of fitting is not satisfactory, which is in accordance with the Williamson–Hall plots, the anisotropic strain broadening is presented in the diffraction patterns of all samples. Therefore, according to the Stephans model, in the interface of Fullprof the following sections were consecutively selected: Microstructre/General Strain Formulation/Broadening Model (Quadratic form). S_{400}, S_{220}, and ζ were also refined along with the other structure and microstructure parameters. It can be seen in Figure 3(b), after refining the anisotropic parameters (S_{400}, S_{220}, and ζ) the fitting quality is significantly improved. Some of the important results are summarized in Tables II and III. Using these values in Eqs. (15) and (16), the fraction of edge dislocation type (η_e) was determined (Table III). In order to determine the dislocation density, the contribution of edge and screw dislocation types on the contrast factor of dislocation must be

TABLE I. Data collection condition.

Sample	Range of scan	Step size (2θ)	Step counting time (s)	Radiation wavelength (Å)	Divergence slits (rad)	Goniometer radius (mm)	Detector type
S_1	40–120	0.02	4	1.789	0.034	173	Scintillation
S_2–S_8	30–120	0.026	60	1.541	0.040	240	Pixel

https://doi.org/10.1017/S0885715616000270 Published online by Cambridge University Press

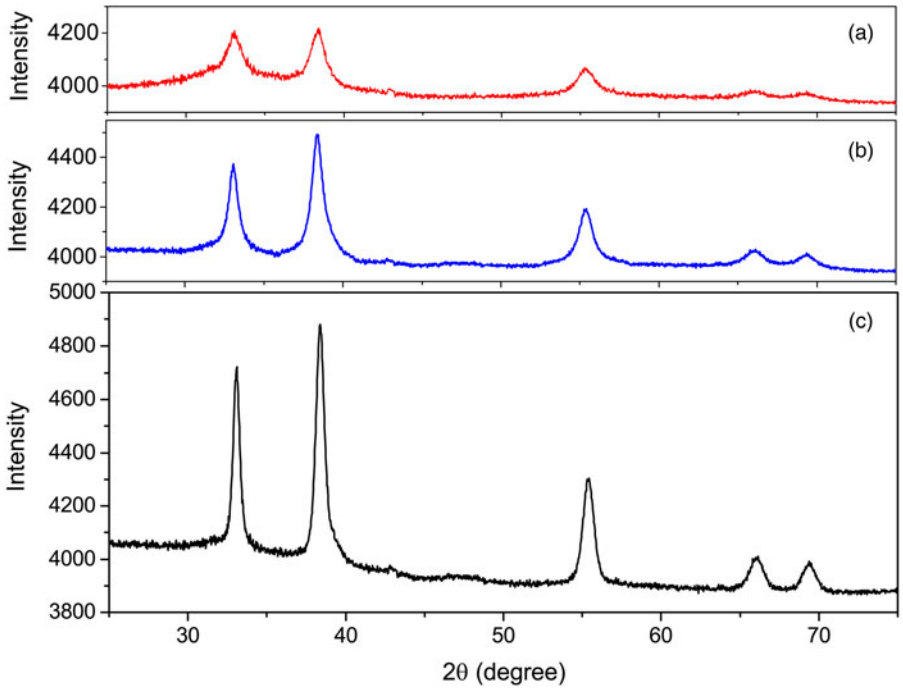


Figure 1. (Color online) The X-ray diffraction patterns of CdO samples annealed at (a) 300, (b) 400 and (c) 500 °C.

identified. To do this, the elastic constants of our crystals were applied and according to the approach described by Ungar *et al*. (1999c), the values of A_e, B_e, A_s, and B_s were determined (Table IV). The details of this procedure are not provided here (see Ungar *et al*., 1999c). These values and η_e were used in Eqs. (11) and (13) and the contrast factor of each reflection was estimated. On the other hand, the dislocation correlation parameter (P) and also the values of Λ were calculated by Eqs. (18) and (19). Finally, by linear fitting to the plots of $\langle e^2 \rangle_{hkl}$ as a function of ξ_{hkl}, the dislocation density of the correspond samples was determined (Figure 4). For better understanding, the parameters used in the above procedure (briefly only the values of Cu phase) are arranged in Table V. The results of samples S_1 to S_3 are added to Table III. The behavior of microstructure parameters corresponding to CdO films (samples S_4 to S_8) are also shown in Figure 5. As is seen in these plots, with the increase of annealing temperature from 300 to 500 °C, the values of crystallite size and lattice constant more or less linearly increase and decrease from 13.8(8) to 26.6 (4) and 0.469 35(3) to 0.469 11(2), respectively. It can also be observed that the dislocation density quadratically decreases from 3.4(6) to 30(2) and the fraction of edge dislocation type only fluctuates from 32(3) to 29(2)%. The CIF formats of the Rietveld refinement procedure corresponding to four different sample types are available in the Supplementary materials.

C. Comparison between the results of Rietveld and WPPM

In the next step, the dislocation results of the Rietveld procedure were compared with those extracted from the WPPM. In the WPPM method, the crystallite size, size distribution behavior, dislocation density (ρ), outer cut-off radius of dislocation (R_e), and the fraction of edge dislocation characters (η_e) can be directly extracted from the diffraction patterns without using any mathematical peak shape function like Voigt or

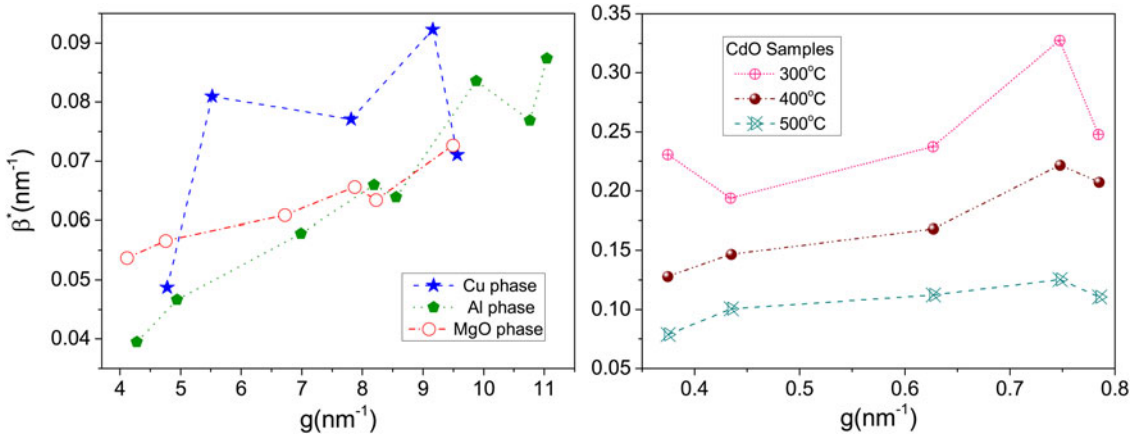


Figure 2. (Color online) The Williamson–Hall plots Cu and Mgo phase which show the variation of β^* versus g.

https://doi.org/10.1017/S0885715616000270 Published online by Cambridge University Press

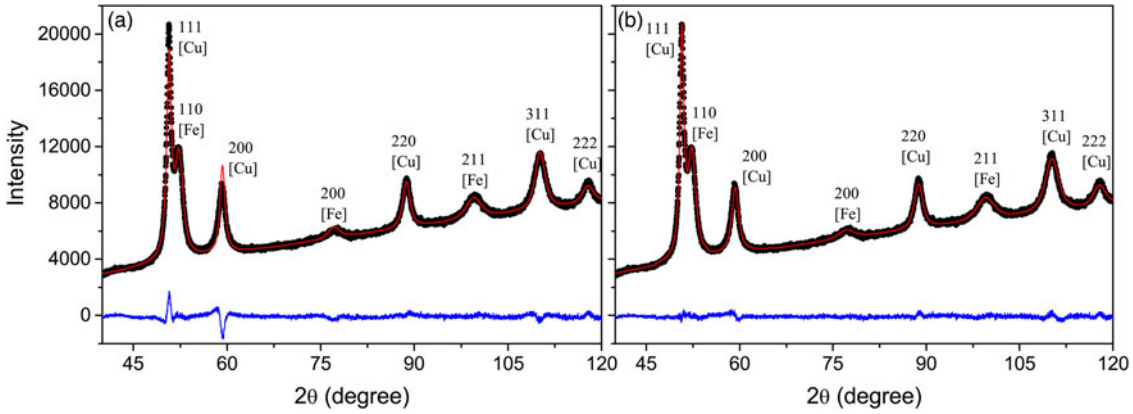


Figure 3. (Color online) The measured and calculated diffraction patterns of sample S_1 by assuming (a) The broadening of reflection is isotrop. (b) The broadening of reflection is anisotrop.

TABLE II. Structure parameters of samples S_1, S_2, and S_3 determined from the Rietveld procedure.

	Sample S_1		Sample S_2	Sample S_3
	Cu	Fe	Al	MgO
Lattice constant (nm)	0.362 053(8)	0.287 237(5)	0.404 902(9)	0.421 713(6)
Phase fractions (%)	57.8(4)	43.2(5)	100	100

TABLE III. Microstructure parameters of samples S_1 and S_2, determined from the Rietveld refinement procedure.

Sample	S_{400}	S_{220}	η_e (%)	D (nm)	$\rho \times 10^{16}$ (m^{-2})
Cu	17(2)	−4.4(4)	19(6)	12(4)	2.02(2)
Fe	19(4)	2.7(3)	63(10)	5(1)	0.89(2)
Al	1.99(3)	1.74(2)	57(7)	45(3)	0.38(4)
MgO	21(2)	18(2)	48(8)	20(2)	0.17(1)

TABLE IV. Parameters of A and B of edge and screw dislocation corresponding to Cu, Fe, Al, MgO, and CdO crystals.

		Edge	Screw
Cu	A	0.3078	0.3035
	B	−0.5177	−0.7274
Fe	A	0.2662	0.2617
	B	−0.3712	−0.7017
Al	A	0.2012	0.1843
	B	−0.0771	−0.2413
MgO	A	0.2091	0.2025
	B	−0.1315	−0.3329
CdO	A	0.2412	0.2869
	B	−0.4935	−0.7320

pseudo-Voigt. The theory of the WPPM procedure has been fully described in (Scardi and Leoni, 2001, 2002); therefore, is not repeated in this study. In this method, by combining the theory of Warren and Averbach (1950) with that proposed by Wilkens (1976), the Fourier coefficients of simulated intensity profiles can be written in terms of the multiplication of Fourier size and Fourier distortion. Since in most of the conditions, the behavior of distribution function can be described by Lognormal function, the size of Fourier coefficient can be written in terms of Lognormal mean (μ), and Lognormal variance (σ) (Scardi and Leoni, 2001). Moreover, the values of contrast factor corresponding to *hkl* reflections are evaluated using Eq. (13) and refining the values of η_e as implemented in PM2 K software (Leoni *et al.*, 2006).

For samples S_1 to S_8, using the PM2K software, the simulated patterns were compared with the measured one and the background coefficients, lattice constants, Lognormal mean, Lognormal variance, outer cut-off radius of dislocation, and the fraction of edge dislocation type were refined using the least-squares method. The procedure was repeated until the difference between the measured and simulated patterns was reduced to minimum. The output results of PM2K (samples S_1 to S_3) are arranged in Table VI. In this table, the value of $\langle D \rangle$ was calculated from Eq. (6) which in this equation, the area $\langle D_A \rangle$ and volume $\langle D_V \rangle$ mean crystallite size, can be determined by applying the values of μ and σ in the following equation:

$$\langle D_A \rangle = \frac{2}{3}\exp(\mu + 2.5\sigma^2) \tag{20}$$

$$\langle D_V \rangle = \frac{3}{4}\exp(\mu + 3.5\sigma^2) \tag{21}$$

The output microstructure results of CdO films are also added to Figure 5. From the plots, one can see that the microstructure behaviors vs. annealing temperature, extracted from Rietveld approximately confirm the results of WPPM approaches. However, as is seen in Tables III and VI and also the plots of Figure 5, the dislocation density and the apparent size of Cu, Al, MgO, and CdO phases corresponding to the Rietveld procedure are higher than those of WPPM. It seems the main reason of these discrepancies is that the contribution of size broadening of each profile in Rietveld is smaller than that of WPPM and therefore compared with the

https://doi.org/10.1017/S0885715616000270 Published online by Cambridge University Press

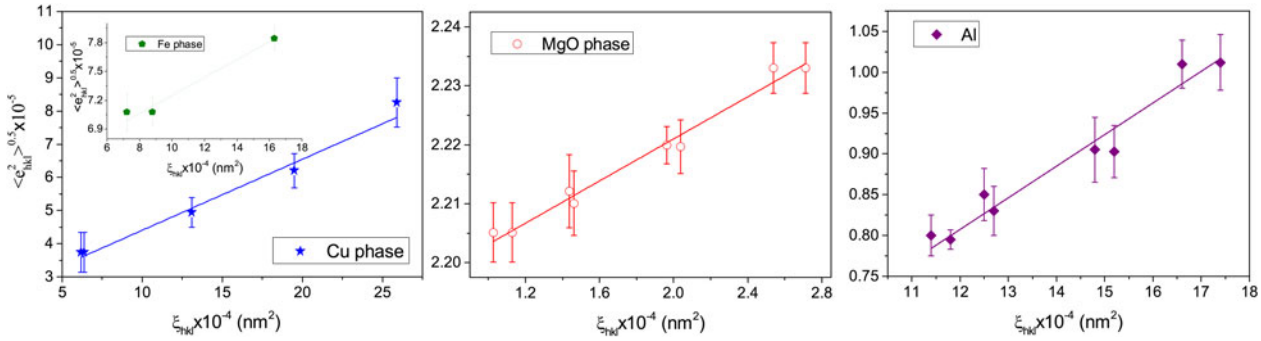


Figure 4. (Color online) The variations of $\langle e^2\rangle_{hkl}$ versus ξ_{hkl} corresponding to Cu, Fe and Mgo phases.

TABLE V. Values of Bragg position, β_G, β_L, P, $\langle e^2\rangle_{hkl}^{1/2}$, and ξ_{hkl} corresponding to Cu phase derived from the Rietveld refinement.

Hkl	2θ	β_G	β_L	P	$\langle e^2\rangle_{hkl}^{1/2}$	ξ_{hkl}
111	50.68	1.72	9.37	0.37	3.7(6)	6.190
200	59.23	3.05	15.57	0.40	8.3(7)	25.900
220	88.67	4.87	13.75	0.72	4.9(5)	13.100
311	110.07	6.14	17.51	0.71	6.2(5)	19.500
222	117.73	6.17	12.77	0.98	3.7(6)	6.356

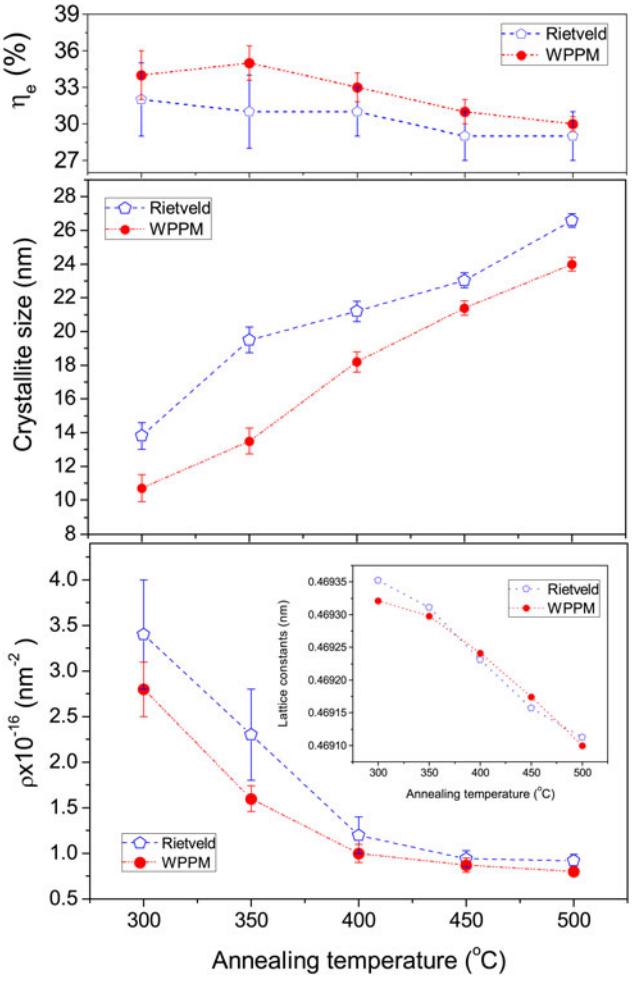


Figure 5. (Color online) Comparison between the behavior of microstructure parameters corresponding to CdO films, extracted by Rietveld and WPPM methods.

WPPM approach, the Rietveld procedure assigns a larger portion of broadening to distortion (lattice defects).The lattice parameters and the fractions of edge dislocation type evaluated by Rietveld, agrees with the results of WPPM.

It should be noted that in the diffraction patterns of sample S_1, Fe phase has only three reflections and the dislocation density determined from the Rietveld method is not sufficiently accurate (see the sub-plot of Figure 4). Because of the simplicity of cubic crystals in this work the linear defects of cubic systems were evaluated; however, for other crystals the above procedure is more complicated.

IV. CONCLUSION

In this study, a method was developed for the extraction of the dislocation characteristics from output values of the Rietveld refinement procedure. The theory of Stephans was combined with the approach introduced by Ungar *et al*. and the fraction of edge dislocation types as well as the dislocation density corresponding to cubic crystals were estimated using the results extracted during the anisotropic strain broadening procedure. The validity of this method was tested by selecting four different nanocrystalline materials, which were synthesized from top-down (mechanical deformed Fe/Cu and Al) and bottom-up (MgO nanopowder and CdO films) techniques. The results of lattice parameters, apparent size, dislocation density, and the fraction of edge dislocation types were then compared with those evaluated by the WPPM method. It is found that not only the lattice parameters and the fraction of edge dislocation character calculated by Rietveld are fairly close to those extracted by WPPM procedure, but also the order of crystallite size and the dislocation density corresponding to Cu, Al, and MgO phases determined from Rietveld are in agreement with the data obtained by WPPM. In CdO thin

https://doi.org/10.1017/S0885715616000270 Published online by Cambridge University Press

TABLE VI. Microstructure parameters determined from the WPPM method.

Sample	a (nm)	μ	σ	η_e (%)	D (nm)	$\rho \times 10^{16}$ (m^{-2})
Cu	0.362 084(9)	1.515(5)	0.593(1)	17(2)	9.6(1)	1.62(2)
Fe	0.287 21(1)	1.55(2)	0.433(5)	54(3)	6.5(2)	3.5(2)
Al	0.404 894(3)	3.835(2)	0.301(5)	59(2)	49.4(9)	0.291(3)
MgO	0.421 516(2)	2.371(2)	0.5112(6)	56(5)	17.9(1)	0.111(2)

films, the behavior of microstructure parameters was studied vs. annealing temperature, using both the Rietveld and WPPM methods, which indicates the results of both methods well confirm each other.

SUPPLEMENTARY MATERIAL

The supplementary material for this article can be found at http://dx.doi.org/10.1017/S0885715616000270.

Attallah, M., Zabeen, S., Cernik, R. J., and Preuss, M. (**2009**). "Comparative determination of the a/b phase fraction in a+b-titanium alloys using X-ray diffraction and electron microscopy," Mater. Charact. **60**, 1248–1256.

Cerny, R., Joubert, J. M., Latroche, M., Percheron, G. A., and Yvon, K. (**2000**). "Anisotropic diffraction peak broadening and dislocation substructure in hydrogen-cycled $LaNi_5$ and substitutional derivatives," J. Appl. Crystallogr. **33**, 997–1005.

Dragomir, I. C. and Ungar, T. (**2002**). "Contrast factors of dislocations in the hexagonal crystal system," J. Appl. Crystallogr. **35**, 556–564.

Ersching, K., Campos, C., Lima, J. C., Grandi, T., Souza, S., and Pizani, P. (**2010**). "X-ray diffraction, Raman and photoacoustic studies of InSb nanocrystals," Mater. Chem. Phys. **122**, 528–532.

Ferrari, M. and Lutterotti, L. (**1994**). "Method for the simultaneous determination of anisotropic residual stresses and texture by x-ray diffraction," J. Appl. Phys. **76**, 7246.

Leoni, M., Confente, T., and Scardi, P. (**2006**). "PM2 K: a flexible program implementing whole powder pattern modelling," Z. Kristallogr. Suppl. **23**, 249–254.

Mojtahedi, M., Goodarzi, M., Aboutalebi, M. R., Ghaffari, M., and Soleimanian, V. (**2013**). "Investigation on the formation of Cu–Fe nano crystalline super-saturated solid solution developed by mechanical alloying," J. Alloys Compd. **550**, 380–388.

Murugesan, S., Kuppusami, P., Mohandas, E., and Vijayalakshmi, M. (**2012**). "X-ray diffraction Rietveld analysis of cold worked austenitic stainless steel," Mater. Lett. **67**, 173–176.

Rahaei, M. B. and Jia, D. (**2014**). "Processing behavior of nanocrystalline NiAl during milling, sintering and mechanical loading and interpretation of its intergranular fracture," Eng. Fract. Mech. **132**, 136–146.

Rietveld, H. M. (**1967**). "Line profiles of neutron powder-diffraction peaks for structure refinement," Acta Crystallogr. **22**, 151–152.

Rodriguez, C. J. (**1990**). "FULLPROF: a program for Rietveld refinement and pattern matching analysis," in *Abstracts of the Satellite Meeting on Powder Diffraction of the XV Congress of the IUCr, International Union of Crystallography*, Toulouse, France, pp. 127.

Sarkar, A., Mukherjee, P., and Barat, P. (**2008**). "Effect of heavy ion irradiation on microstructure of zirconium alloy characterised by X-ray diffraction," J. Nucl. Mater. **372**, 285–292.

Scardi, P. and Leoni, M. (**2001**). "Diffraction line profiles from polydisperse crystalline systems," Acta Crystallogr. A **57**, 604–613.

Scardi, P. and Leoni, M. (**2002**). "Whole powder pattern modeling," Acta Crystallogr. A **58**, 190–200.

Soleimanian, V. and Mojtahedi, M. (**2015**). "A comparison between different X-ray diffraction line broadening analysis methods for nanocrystalline ball-milled FCC powders," Appl. Phys. A **119**, 977–987.

Soleimanian, V., Abedi, M., and Aghdaee, S. R. (**2015**). "Microstructure evaluation of nanocrystalline MgO powders using the advanced X-ray line profileanalysis," J. Cryst. Growth **411**, 4–11.

Solovyov, L. A. (**2000**). "A correction for anisotropic line broadening due to structural defects in powder diffraction structure analysis," J. Appl. Crystallogr. **33**, 338–343.

Stephens, P. W. (**1999**) "Phenomenological model of anisotropic peak broadening in powder diffraction," J. Appl. Crystallogr. **32**, 281–289.

Ungar, T. and Tichy, G. (**1999b**). "The effect of dislocation contrast on X-ray line profiles in untextured polycrystals," Phys. Status Solidi A **171**, 425–434.

Ungar, T., Leoni, M., and Scardi, P. (**1999a**). "The dislocation model of strain anisotropy in whole powder-pattern fitting: the case of a Li–Mn cubic spinel," J. Appl. Crystallogr. **32**, 290–295.

Ungar, T., Dragomir, I., Revesz, A., and Borbely, A. (**1999c**) "The contrast factors of dislocations in cubic crystals: the dislocation model of strainanisotropy in practice," J. Appl. Crystallogr. **32**, 992–1002.

Warren, B. E. and Averbach, B. L. (**1950**). "The effect of cold-work distortion on X-ray patterns," J. Appl. Phys. **21**, 595–599.

Wilkens, M. (**1976**). "Broadening of X-ray diffraction lines of crystals containing dislocation distributions," Kristallogr. Tech. **11**, 1159–1169.

Williamson, G. K. and Hall, W. H. (**1953**). "X-ray line broadening from filed aluminium and wolfram," Acta Metall. **1**, 22–31.

Williamson, G. K. and Smallman, R. E. (**1956**). "Dislocation densities in some annealed and cold-worked metals from measurements on the X-ray debye-scherrer spectrum" Philos. Mag. **1**, 34–46.

Wu, E., Gray, E. and MacA, K. E. H. (**1998a**). "Modelling dislocation-induced anisotropic line broadening in rietveld refinements using a Voigt function. I. General principles," J. Appl. Crystallogr. **31**, 356–362.

Wu, E., Kisi, E. H. and Gray, E. M. (**1998b**). "Modelling dislocation-induced anisotropic line broadening in rietveld refinements using a Voigt function. II. Application to neutron powder diffraction data," J. Appl. Crystallogr. **31**, 363–368.

Yahia, I. S., Salem, G. F., Abd, M. S., and Yakuphanoglu, F. "Optical properties of Al-CdO nano-clusters thin films," Superlattice Microstruct. **64** (**2013**), 178–184.

Zhang, Z., Jiang, C., Fu, P., Cai, F., and Ma, N. (**2015**). "Microstructure and texture of electrodeposited Ni–ZrC composite coatings investigated by Rietveld XRD line profile analysis," J. Alloys Compd. **625**, 118–123.

https://doi.org/10.1017/S0885715616000270 Published online by Cambridge University Press